Submitted conference paper (last modification: 7-July-2003):

Michael Buchwitz and John P. Burrows,
Retrieval of CH_4, CO, and CO_2 total column amounts from SCIAMACHY near-infrared nadir spectra: Retrieval algorithm and first results,
to be presented at: SPIE 10^{th} International Symposium "Remote Sensing",
8-12 September 2003, Barcelona, Spain,
Conference 5235 "Remote Sensing of Clouds and the Atmosphere VIII",
to be published in Proceedings of SPIE Volume 5235

Copyright 2003 Society of Photo-Optical Instrumentation Engineers.
This paper will be published and is made available as an electronic preprint with permission of SPIE. One print or electronic copy may be made for personal use only. Systematic or multiple reproduction, distribution to multiple locations via electronic or other means, duplication of any material in this paper for a fee or for commercial purposes, or modifications of the content of the paper are prohibited.

Retrieval of CH_4, CO, and CO_2 total column amounts from SCIAMACHY near-infrared nadir spectra: Retrieval algorithm and first results

Michael Buchwitz and John P. Burrows

Institute of Environmental Physics (iup) / Institute of Remote Sensing (ife), University of Bremen, Bremen, Germany

ABSTRACT

SCIAMACHY is a UV/visible/near-infrared grating spectrometer on board the European environmental satellite ENVISAT that observes the atmosphere in nadir, limb, and solar and lunar occultation viewing geometries with moderate spectral resolution (0.2-1.5 nm). At the University of Bremen a modified DOAS algorithm (WFM-DOAS) is being developed primarily for the retrieval of CH_4, CO, CO_2, H_2O, N_2O, and O_2 total columns from SCIAMACHY near-infrared and visible nadir spectra. A first version of this algorithm has been implemented based on a fast look-up table approach. The algorithm and the look-up table is described along with an initial error analysis. Weighting functions and averaging kernels indicate that the SCIAMACHY near-infrared nadir measurements are highly sensitive to trace gas concentration changes even in the lowest kilometer of the atmosphere. The results presented have been obtained by applying WFM-DOAS to small spectral fitting windows focusing on CH_4, CO_2, CO, and O_2 column retrieval and CH_4 and CO_2 to O_2 column ratios (denoted XCH_4 and XCO_2, respectively). These type of data products are planned to be used within the EU research project EVERGREEN to constrain surface sources and sinks of CH_4 and CO_2 using inverse modeling techniques. This study discusses the first set of WFM-DOAS products generated for and to be further improved within EVERGREEN. Although no detailed validation has been performed yet we found that the retrieved columns have the right order of magnitude and show (at least qualitatively) the expected correlation of the well mixed gases CO_2 and CH_4 with O_2 and surface topography. The standard deviation of the dry air column averaged mixing ratio XCO_2 within 10° latitude bands is $\pm$10 ppmv or $\pm$2.7% (XCH_4: $\pm$50 ppbv or $\pm$2.8%) for measurements over land (over ocean the scatter is a factor of 2-4 larger). These values have been determined from $\sim$25% of the ground pixels of one orbit which fulfill the following requirements: (nearly) cloud free, solar zenith angle $< 75°$, XCO_2 error $< 4\%$ (XCH_4 error $< 6\%$). It has not yet been assessed how much of this variability can be attributed to real column changes. The observed variability is about three times larger than expected from (single spectra) signal-to-noise considerations but might be affected by limitations of the current implementation of the retrieval algorithm (e.g., sensitivity to surface reflectivity) and calibration issues (e.g., not yet considered ADC non-linearity correction). Especially the CO retrieval needs further study and improvement. The CO fit errors are 20-40% over land but typically significantly larger over the ocean. A clear identification of the weak CO lines is difficult as the CO fit residuals are dominated by relatively stable systematic artifacts (also observed in the CO_2 and CH_4 fitting windows) on the order of the weak CO absorption lines. This might be explained by the still preliminary calibration of the SCIAMACHY spectra and/or errors of the spectroscopic data.

Keywords: Remote sensing, near infrared, troposphere, trace gases, greenhouse gases, biogeochemical cycles

1. INTRODUCTION

WFM-DOAS (Weighting Function Modified Differential Optical Absorption Spectroscopy) is a modified DOAS algorithm[1] under development at the University of Bremen mainly for the retrieval of trace gas columns from SCIAMACHY[2] and GOME/ERS-2[3] nadir radiance and solar irradiance spectra. WFM-DOAS is independent of the official ESA/DLR ENVISAT operational Level 1 to 2 algorithms and Level 2 data products[2] and scientific algorithms developed at other

Further author information: (Send correspondence to M.B.)

M.B.: E-mail: Michael.Buchwitz@iup.physik.uni-bremen.de, Telephone: +49 (0)421 218 4475

J.P.B.: E-mail: burrows@iup.physik.uni-bremen.de, Telephone: +49 (0)421 218 4548, Address: University of Bremen FB1, Institute of Environmental Physics (iup), Otto Hahn Allee 1, P.O. Box 330440, D-28334 Bremen, Germany

institutions[4–6] which are not discussed here. The term vertical column amount refers to the vertically integrated concentration profile of a given trace gas (in number of molecules per unit area). Analysis of simulated SCIAMACHY near-infrared (NIR) nadir measurements prior to the launch of ENVISAT indicated that the retrieval precision (defined as column error resulting from instrument noise) is about 1% for the strong NIR absorbers CH_4, CO_2, and H_2O, and about 10% for the weak NIR absorbers CO and N_2O (assuming an integration time of 1 s and the use of entire channels rather than small spectral micro-windows for retrieval).[1,7] In order to obtain retrieval accuracies on this order, systematic retrieval errors (bias) resulting from, e.g., calibration errors or retrieval algorithm limitations, need to be minimized as much as possible. Accuracies/precisions on the order of 1% for single (O_2 normalized) CH_4 and CO_2 columns are needed if the data are to be used for scientific applications such as constraining CH_4 and CO_2 surface sources and sinks[8–10] as planned, e.g., within the EU 5^{th} framework research project EVERGREEN (`http://www.knmi.nl/EVERGREEN/`). On the other hand the retrieval algorithm also has to be very fast in order to process huge amounts of data. In practise this means that an acceptable compromise between accuracy and speed has to be found. In this study initial results concerning the application of a first version of this algorithm to SCIAMACHY Level 1c (i.e., calibrated) nadir and solar spectra are presented.

2. DESCRIPTION OF THE WFM-DOAS RETRIEVAL ALGORITHM

WFM-DOAS is based on fitting the logarithm of a linearized radiative transfer model I_i^{mod} plus a low-order polynomial P_i to the logarithm of the ratio of a measured nadir radiance and solar irradiance spectrum, i.e., observed sun-normalized radiance I_i^{obs}. Index i refers to the center wavelength λ_i of (linear diode array) detector pixel number i. Provided there exists an appropriate spectral fitting window, I_i^{obs} depends on the true but unknown vertical columns of the trace gases of interest (components of vector $\mathbf{V}^t$). The WFM-DOAS equation can be written as follows:

$$\left\| \ln\, I_i^{obs}(\mathbf{V}^t) \;-\; \left[\ln I_i^{mod}(\bar{\mathbf{V}}) + \sum_{j=1}^{J} \left.\frac{\partial \ln I_i^{mod}}{\partial V_j}\right|_{\bar{V}_j} \times (\underline{\hat{V}_j} - \bar{V}_j) + \; P_i(\underline{a_m}) \right] \right\|^2 \equiv \|RES_i\|^2 \;\rightarrow\; min. \qquad (1)$$

A derivative, or weighting function, with respect to a vertical column refers to the change of the radiance due to a change (scaling) of a pre-selected trace gas vertical profile. To simplify the notation, the dependence of the radiance on other important parameters (e.g., temperature profile or albedo) has been omitted in Eq. (1). In the following the term in square brackets is called the WFM-DOAS model. The WFM-DOAS reference spectra are the logarithm of the sun-normalized radiance and its derivatives. They are computed with a radiative transfer model[11] for assumed (e.g., climatological) "mean" columns $\bar{\mathbf{V}}$. Multiple scattering is fully taken into account. The fit parameters (underlined in Eq. (1)) are the desired trace gas vertical columns $\hat{V}_j$ and the polynomial coefficients a_m. Additional fit parameters also used in this study are temperature profile shift and surface albedo change. The fit parameter values are determined by minimizing (in least-squares sense) the difference between observation and WFM-DOAS model, i.e., fit residuum RES_i. The least-squares problem (Eq. (1)) can also be expressed in the following vector/matrix notation: Minimize $\|\mathbf{y} - \mathbf{A}\,\mathbf{x}\|^2$ with respect to $\mathbf{x}$. The solution is $\hat{\mathbf{x}} \;=\; \mathbf{C_x}\,\mathbf{A}^T\mathbf{y}$ where $\mathbf{C_x} \;\equiv\; (\mathbf{A}^T\mathbf{A})^{-1}$ is the covariance matrix of solution $\hat{\mathbf{x}}$. The errors of the retrieved columns reported in this study (e.g., error bars Fig. 18) have been calculated as follows[12]: $\sigma_{\hat{V}_j} \;=\; \sqrt{(\mathbf{C_x})_{jj} \times \sum_i RES_i^2/(m\; - \; n)}$, where $(\mathbf{C_x})_{jj}$ is the j-th diagonal element of the covariance matrix, m is the number of spectral points in the fitting window (typically 100) and n is the number of linear fit parameters (typically 6).

In order to avoid time consuming on-line radiative transfer simulations, a look-up table approach has been implemented. The WFM-DOAS reference spectra (radiance and derivatives) have been computed for cloud free conditions assuming a US Standard Atmosphere (CH_4 and CO_2 were scaled to current concentrations) a tropospheric maritime and stratospheric background aerosol scenario and a surface albedo of 0.1. The tabulated reference spectra depend on solar zenith angle (SZA: 0°-90° in steps of 5°), surface elevation (0, 1, 2, 3 km) and water vapor column (scaling factors: 0.5, 1.0, 1.5, 2.0, 4.0), in total 400 combinations. WFM-DOAS has been implemented as an iterative scheme, mainly to account for non-linearities introduced by the high variability of atmospheric water vapor (initial guess: scaling factor 1.0, i.e., unchanged US Standard Atmosphere water vapor profile).

3. SPECTRAL FITTING WINDOWS

The results shown in this study mainly refer to five rather narrow spectral fitting windows listed in Table 1. This means that for this study only a small sub-set of the spectral information of the SCIAMACHY measurements has been used for retrieval. The spectral fitting windows have been selected as a starting point for retrieval algorithm investigation and optimization. Currently, the calibration of the SCIAMACHY spectra is still preliminary (e.g., with respect to polarization correction, pixel-to-pixel gain correction, analog-to-digital converter (ADC) non-linearity correction). It is expected that the fitting windows can be significantly enlarged - thereby improving the precision - once the calibration has been improved in operational Level 0 to 1 processing (this requires a processor upgrade (expected for end of 2003) and reprocessing of the archived Level 0 data). Table 1 also lists the default fit parameters used in this study, except the coefficients of the low order polynomial which is always included. Among the criteria for selecting the fitting windows was to minimize interference with water vapor absorption. Therefore, H_2O columns are currently only retrieved as a by-product of low quality (it is planned to generate an accurate H_2O column SCIAMACHY WFM-DOAS data product in the near future). When testing an early implementation of WFM-DOAS prior to the launch of ENVISAT H_2O columns of good quality have been retrieved from GOME/ERS-2[3] spectra at 700 nm.[13]

The spatial (horizontal) resolution of the SCIAMACHY nadir measurements depends on orbital position and spectral interval.[2] Low solar zenith angles (e.g., tropical and sub-tropical regions) correspond to best (smallest) spatial resolution. The ground pixel (footprint) size for fitting windows WIN_CH_4 and WIN_CH_6 is (nearly) identical at each orbital position: 60×30 km^2 for an integration times of 0.25 s and 120×30 km^2 for 0.5 s (these integration times cover most of the orbit). For the channel 7 and 8 fitting windows the footprint size is typically a factor of two larger (120×30 km^2 (0.5 s) and 240×30 km^2 (1.0 s)).

For the spectral fitting windows used in this study SCIAMACHY instrument signal-to-noise (S/N) calculations for simulated nadir radiances corresponding to a solar zenith angle of 50° and a surface albedo of 0.1 in combination with WFM-DOAS retrievals have been performed. The results are also shown in Tab. 1. The channel 7 and 8 S/N and precision values are valid for nominal transmission, i.e., without consideration of any (temporal) transmission degradation due to (reversible) ice build up on the SCIAMACHY detectors. Note that S/N and the retrieval precisions are roughly proportional to the measured signal (after dark signal correction) which is in turn (approximately) proportional to transmission (and other important parameters such as surface albedo).

Table 1. Overview of the spectral fitting windows and main retrieval parameters used in this study (first four columns). The last two columns indicate the performance of these channels in terms of signal-to-noise ratios and retrieval precisions. S/N is the average signal-to-noise-ratio (valid for a solar zenith angle of 50° and an albedo of 0.1) given for two integration times (value before colon, unit is seconds). Precision is the 1-sigma trace gas column retrieval precision of the main fit parameter for the given S/N performance.

ID / Channel	Spectral interval [nm]	Main fit parameter	Additional fit parameter (default)	S/N [-]	Precision of main fit parameter [%]
WIN_CH_4 / 4	755 - 775	O_2 column	Temp., albedo	N.A. ($>$ 1000)	N.A. ($<$ 1%)
WIN_CH_6 / 6	1558 - 1594	CO_2 column	H_2O, temp.	0.25: 670, 0.5: 1100	0.25: 1.0, 0.5: 0.6
WIN_CH_7 / 7	2030 - 2040	CO_2 column	H_2O, temp.	0.50: 260, 1.0: 390	0.50: 1.4, 1.0: 0.9
WIN_CH_8a / 8	2265 - 2280	CH_4 column	N_2O, H_2O, temp.	0.50: 140, 1.0: 200	0.50: 1.1, 1.0: 0.7
WIN_CH_8b / 8	2359 - 2370	CO column	CH_4, H_2O, temp.	0.50: 50, 1.0: 70	0.50: 19, 1.0: 13

4. WEIGHTING FUNCTIONS AND AVERAGING KERNELS

The advantage of the near-infrared spectral region, in contrast to the, e.g., UV or the thermal infrared regions, is that the radiation detected by a nadir viewing satellite instrument is highly sensitive with respect to the trace gas concentrations even in the lowest kilometer of the atmosphere. This is demonstrated in this section for SCIAMACHY observations. For this purpose simulated nadir spectra have been generated for an unperturbed (US Standard) atmosphere as well as for perturbed atmospheres where a certain (constant) number of (CH_4, CO_2, and CO) molecules have been added at various altitude levels. Typical results are displayed in Figure 1 showing the radiance sensitivity due to CH_4 concentration changes. As can be seen, the radiance is sensitive even to concentration changes at the bottom of the atmosphere (0 km). The sensitivity per CH_4 molecule increases with decreasing altitude. This seems to be typical for strong absorption lines and also is observed for CO_2 (saturation of unresolved lines in the strong absorber limit,[14] see also next paragraph). CO shows an opposite behavior (the CO lines are weak), namely a slight decrease of sensitivity with decreasing perturbation altitude.

In order to determine how the retrieved column depends on the profile of the trace gas to be retrieved, Figures 2-4 show so-called vertical column averaging kernels (AK) for CH_4, CO_2, and CO, respectively. They are defined as follows:

$AK(z) \equiv (V^{rp} - V^{tu})/(V^{tp} - V^{tu})$, where V^{tu} is the $t$rue column of the trace gas considered for the $u$nperturbed vertical profile, and V^{tp} and V^{rp} are the $t$rue and $r$etrieved columns of the $p$erturbed profile (enhanced concentration at altitude z km), respectively. The averaging kernels have been computed by applying WFM-DOAS to synthetic radiance spectra. In line with the discussion of Figure 1, the retrieval sensitivity for CH_4 and CO_2 increases with decreasing perturbation altitude. Dufour and Bréon[15] have presented a similar result to that shown in Figure 3 for CO_2 but for higher spectral resolution. This increase of sensitivity is advantageous for CH_4 and CO_2 source/sink determination as most of the information on local sources and sinks is located close to the Earth's surface.

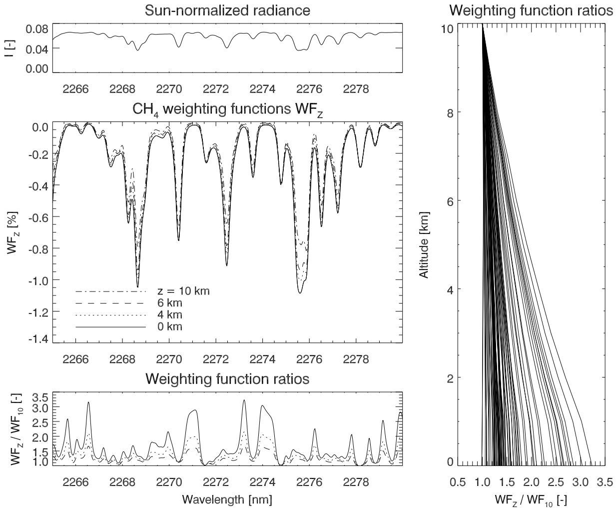

Fig. 1. Left: Top: Sun-normalized radiance (SZA 50°, albedo 0.1). Middle: Relative difference of radiance spectra (weighting functions) calculated for perturbed profiles (perturbation at z km corresponding to a +2% CH_4 column change) and the unperturbed CH_4 profiles. Bottom: Ratios of weighting functions with the weighting function for a perturbation at 10 km. Right: As bottom left but different representation (each line corresponds to one wavelength).

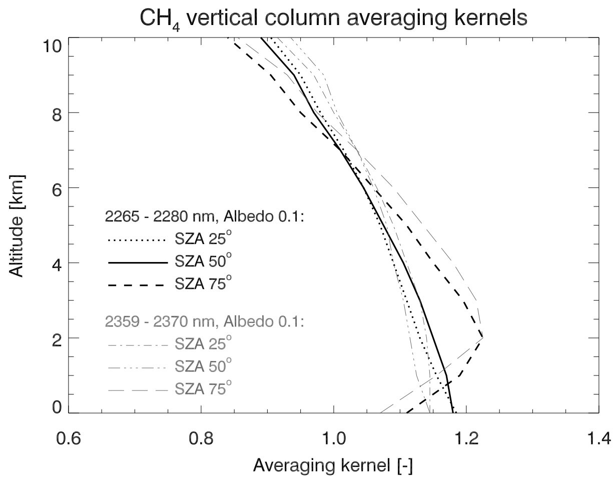

Fig. 2. CH_4 vertical column averaging kernels obtained by applying the WFM-DOAS retrieval algorithm to spectra as shown in Figure 1 (fitting windows: WIN_CH_8a and WIN_CH_8b).

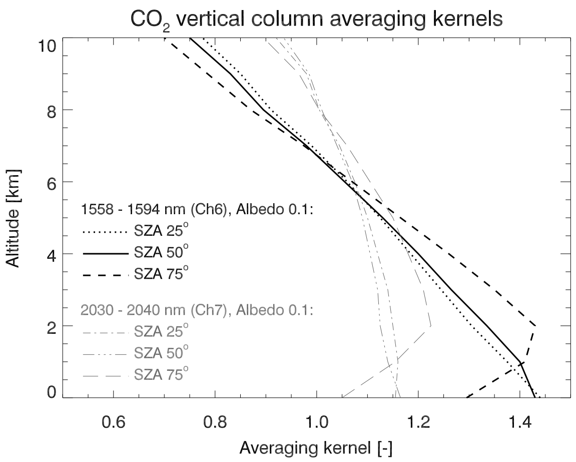

Fig. 3. CO_2 vertical column averaging kernels (for WIN_CH_6 and WIN_CH_7).

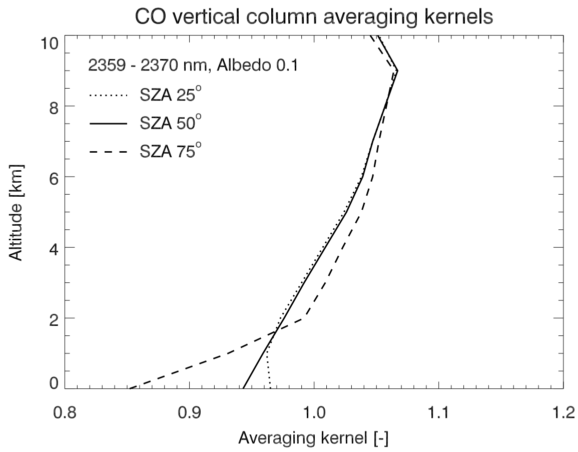

Fig. 4. CO vertical column averaging kernels (WIN_CH_8b).

5. WFM-DOAS ERROR ANALYSIS

The fast look-up table approach introduces errors. In addition, there are errors resulting from parameters that influence the radiative transfer but are not retrieved by WFM-DOAS, such as aerosols and clouds. In the following, an initial error analysis of the currently implemented version of WFM-DOAS is presented. For this purpose, simulated nadir spectra have been generated with a radiative transfer model for various conditions, such as different model atmospheres and surface albedos. If not stated otherwise, the results shown in this section are valid for a solar zenith angle of 50° and albedo 0.1.

5.1. Sensitivity to vertical profiles

The currently implemented look-up table has been generated assuming vertical profiles of pressure, temperature and trace gas volume mixing ratios corresponding to the US Standard Atmosphere (CH_4 and CO_2 concentrations scaled to 1750 ppbv and 370 ppmv, respectively). In order to estimate the vertical column retrieval errors resulting from applying WFM-DOAS to different atmospheres, simulated spectra for several model atmospheres have been generated. The results are shown in Table 2. The retrieval errors mainly reflect the difference in temperature and water vapor profiles of the various atmospheres compared to the US Standard (USS) reference atmosphere (Temperatures at sea level: USS 288.1 K, SAW 257.2 K, TRO 299.7 K; H_2O columns in g/cm^2: USS 1.43, SAS 0.21, TRO 4.18). As can be seen, if a temperature profile shift is included in the fit, the errors are on the order of 1-2%, except for CO, where the error can be as large as nearly 10%.

Table 2. Vertical column retrieval errors resulting from applying WFM-DOAS to spectra generated using various model atmospheres. The values given in brackets refer to retrievals without allowing for a temperature profile shift in the retrieval.

Atmosphere	WIN_CH_8a CH_4 [%]	WIN_CH_8b CO [%]	WIN_CH_6 CO_2 [%]	WIN_CH_7 CO_2 [%]	WIN_CH_4 O_2 [%]
Sub-arctic summmer (SAS)	1.3 (0.8)	0.1 (1.8)	0.0 (-0.8)	0.6 (3.9)	0.0 (-1.7)
Sub-arctic winter (SAW)	1.1 (5.1)	1.8 (-12.8)	0.1 (4.3)	-1.7 (22.3)	0.4 (10.8)
Mid-latitude summer (MLS)	0.9 (-1.0)	-4.6 (21.5)	-0.1 (-2.5)	-0.2 (15.3)	0.1 (-5.4)
Mid-latitude winter (MLW)	1.2 (3.0)	0.7 (-10.8)	0.4 (2.3)	0.0 (11.0)	0.8 (5.4)
Tropical (TRO)	-0.4 (-2.6)	-8.6 (35.8)	-0.4 (-3.0)	-2.3 (20.5)	0.0 (-6.6)

5.2. Sensitivity to aerosols and subvisual cirrus clouds

Aerosols and clouds mainly scatter but also absorb solar radiation. The bulk of the gases relevant for this study is situated in the lowest kilometers of the atmosphere, i.e., in a region where clouds and aerosols are present in extremely variable type and concentration. The look-up table used in this study has been generated using a single aerosol scenario only. It is based on the aerosol parameterization also implemented in the radiative transfer model MODTRAN based on work done by Shettle and Fenn.[16] This (default) scenario can be characterized as follows: Maritime aerosol in the boundary layer (BL), tropospheric visibility and relative humidity 23 km and 80%, respectively, and background stratospheric and normal mesospheric conditions. Aerosol scattering and absorption vertical optical depth are listed in Table 3. To a first approximation aerosols increase or decrease the overall (i.e., spectrally broadband) level of solar radiation scattered back to space. This effect is taken into account by the polynomial included in Eq. (1). However, aerosols also determine the relative depth of absorption lines by influencing the (average) photon path.

The retrieval error due to aerosol has been estimated by defining several (including two rather extreme) aerosol scenarios (see Tables 3 and 4). The "OPAC average continental" aerosol scenario[17] and radiative transfer simulations differ from the default scenario used for the reference spectra in various aspects (Mie phase function instead of Henyey-Greenstein approximation, scattering and extinction profiles). "OPAC average continental" aerosol consists of a mixture of "water soluble aerosol" (small particles mainly originating from gas-to-particle conversion), soot, and "insoluble aerosol" (dust). The "Enhanced aerosol in boundary layer (BL)" scenario contains urban aerosol in the BL with a visibility as low as 2 km and a high relative humidity of 99%. For the "No aerosol in atmosphere" scenario the aerosols have been entirely "switched off" in the radiative transfer simulation. Table 4 shows that WFM-DOAS as applied to NIR spectra appears to be rather insensitive to aerosols ($<$ 1%). In the visible (O_2 A-band) the sensitivity is, however, significantly larger.

No attempts have been made so far to extend WFM-DOAS by a cloud correction scheme in order to deal with clouds (e.g., partial cloud cover or thin clouds). The current approach is based on identification (and elimination) of cloud contaminated ground pixels. SCIAMACHY offers various possibilities for cloud detection, even on sub-pixel scale. In this study a very simple threshold algorithm is used based on SCIAMACHY's UV PMD (Polarization Measurement Device) measurements.[2] Even with a more sophisticated algorithm it might not be possible to identify all cloud contaminated pixels. A certain level of cloud contamination might even be tolerated in order to increase the number of useful measurements. In this context it is interesting to estimate the vertical column retrieval error resulting from (undetected) subvisual cirrus clouds. These clouds are predominantly a tropical/subtropical phenomenon. Cirrus clouds have been modeled in this study as a scattering layer of 1 km vertical extent centered at 12 km. The assumed scattering vertical optical depths were 0.01, 0.02, and 0.03 independent of wavelength. This is a reasonable assumption because the particles are much larger than the wavelength considered here. A scattering optical depth of 0.03 roughly corresponds to the maximum optical depth of subvisual cirrus clouds at 500 nm. Table 4 shows that such a scattering layer near the tropopause is expected to lead to an underestimation of the retrieved vertical columns (shielding of the troposphere lying underneath) by more than 1% in most cases. The values listed in Table 4 for the underestimation of the retrieved CO_2 column in the presence of cirrus clouds are similar as the values reported in Dufour and Bréon.[15] For an optical depth of 0.03 they estimated this error to be -1.0% (here: -1.4%) at 1.6 microns and -2.0% (here: -3.7%) at 2.0 microns. Identical values are not to be expected because of the different spectral resolution and spectral intervals used in both studies. Concerning aerosols they also found similar errors ($<$ 1.5 ppmv (or 0.4%)) as given in Table 4 for CO_2.

Table 3. Aerosol scattering (ASOD) and absorption vertical optical depth (AAOD) for the aerosol scenarios defined for this error analysis (see also Table 4). Rayleigh scattering vertical optical depth (RSOD) has been included for comparison.

Aerosol scenario		500 nm	750 nm	1500 nm	2000 nm	2300 nm
Look-up table default:	ASOD:	0.305	0.2475	0.17748	0.14933	0.13506
	AAOD:	0.004	0.0029	0.00307	0.00342	0.00258
	RSOD:	0.144	0.0276	0.00170	0.00054	0.00031
OPAC average continental:	ASOD:	0.292	0.1680	0.06200	0.04071	0.03225
	AAOD:	0.032	0.0239	0.01542	0.00981	0.00898
Enhanced aerosol in BL:	ASOD:	2.859	2.1393	0.97306	0.65477	0.53859
	AAOD:	0.195	0.1338	0.08092	0.07498	0.06101

Table 4. Vertical column retrieval errors resulting from aerosol variability and undetected subvisual cirrus clouds at 12 km (OD means scattering optical depth). The values in brackets are valid for retrievals where the albedo weighting function has been included in the fit (except for O_2 where the albedo weighting function has been excluded).

Aerosol/cloud scenario	WIN_CH_8a CH_4 [%]	WIN_CH_8b CO [%]	WIN_CH_6 CO_2 [%]	WIN_CH_7 CO_2 [%]	WIN_CH_4 O_2 [%]
Aerosol:					
OPAC average continental	-0.3 (-0.5)	-0.5 (-0.8)	-0.5 (-0.1)	-0.2 (-0.8)	-0.5 (-2.2)
Enhanced aerosol in BL	-0.2 (0.3)	0.8 (1.6)	-0.9 (0.4)	-0.8 (1.4)	6.1 (4.1)
No aerosol in atmosphere	-0.3 (-0.8)	-0.6 (-1.2)	-0.8 (-1.0)	-0.1 (-1.4)	-2.5 (2.4)
Clouds:					
Subvisual cirrus (OD 0.01)	-1.1 (1.7)	-1.4 (0.4)	-0.4 (1.7)	-1.2 (0.4)	1.1 (-2.7)
Subvisual cirrus (OD 0.02)	-2.4 (3.2)	-2.8 (0.7)	-0.8 (3.1)	-2.4 (0.6)	2.0 (-5.4)
Subvisual cirrus (OD 0.03)	-3.7 (4.5)	-4.0 (0.9)	-1.4 (4.2)	-3.7 (0.8)	2.8 (-8.1)

5.3. Sensitivity to surface albedo

The WFM–DOAS look-up table used in this study has been generated assuming a constant (Lambertian) albedo of 0.1. To a first approximation albedo affects the overall (i.e., spectrally broadband) level of solar radiation scattered back to space. This effect is taken into account by the polynomial included in Eq. (1). However, as aerosols, the albedo also influences the relative depth of absorption lines. As shown in Table 5 the retrieval errors might exceed 1%, especially if no albedo weighting function is included in the fit. The albedo sensitivity in the spectral region of the oxygen A-band is significantly higher than in the near-infrared spectral region (as scattering is more important at shorter wavelength), especially if no albedo weighting function is included. Therefore, albedo is included in the fit (see Table 1) despite the high correlation with the O_2 absorption (correlation coefficient $\sim$0.95). Note that in principle the albedo sensitivity can be reduced simply by extending the look-up table and by estimating the albedo from the SCIAMACHY spectra in spectral regions relatively free of gas absorption (future work, assumes cloud free pixels). Table 5 shows that the retrieval errors are less than a few percent except for very low albedo scenes, even if the albedo weighting function is not included in the fit. Dufour and Bréon[15] compiled a list of surface reflectances for the spectral regions 1.6 and 2.0 microns. According to their Table 2 the surface reflectance of vegetation is 0.18 (desert: 0.4, snow/ice: 0.15) at 1.6 microns and 0.1 at 2.0 microns (desert: 0.35, snow/ice: 0.02). Concerning the specular component of the ocean reflectance (sun glint condition) they report values larger than approximately 0.2 for a solar zenith angle of 40° and wind speeds below 10 m/s but point out that the diffuse component of the reflected light in the infrared is very small ("less than 0.001").

Table 5. Vertical column retrieval errors as a function of surface albedo. For an albedo of 0.1 the errors are zero because the reference spectra are calculated for albedo 0.1. The values in brackets are valid for retrievals where the albedo weighting function has been included in the fit (except for O_2 where the albedo weighting function has been excluded).

Albedo	WIN_CH_8a CH_4 [%]	WIN_CH_8b CO [%]	WIN_CH_6 CO_2 [%]	WIN_CH_7 CO_2 [%]	WIN_CH_4 O_2 [%]
0.30	0.8 (0.1)	0.6 (0.2)	1.4 (0.5)	0.9 (0.3)	-3.0 (22.8)
0.20	0.5 (0.0)	0.4 (0.1)	0.9 (0.3)	0.6 (0.1)	-1.5 (15.5)
0.10	0.0 (0.0)	0.0 (0.0)	0.0 (0.0)	0.0 (0.0)	0.0 (0.0)
0.05	-0.7 (0.0)	-0.4 (0.1)	-1.3 (0.3)	-1.0 (0.1)	-2.1 (-17.9)
0.03	-1.5 (0.1)	-0.8 (0.2)	-2.6 (-0.4)	-2.0 (0.2)	-6.3 (-30.7)
0.003	-7.4 (0.8)	-8.2 (0.4)	-10.3 (1.3)	-9.0 (1.2)	-25.8 (-62.2)

5.4. Other error sources

In this section three additional errors are quantified which are related to the (rather sparse) grid selected for the reference spectra look-up table: solar zenith angle interpolation, scan angle correction, surface elevation (pressure). Note that these errors can be reduced relatively easily, e.g., by extending the look-up table.

The WFM-DOAS look-up table used in this study has been generated for a range of solar zenith angles from 0 to 90° in steps of 5°. These spectra are interpolated to the solar zenith angle of the measurement. The resulting retrieval error is rather small (e.g., less than 0.03% for a solar zenith angle of 52.4°). The look-up table has been generated for exact nadir observation only, neglecting the ±30° scan around the nadir direction. The columns as determined by the fit are corrected using a simple geometrical approximation[1] to account for the enhancement of the depth of absorption lines due to the slant path viewing geometry. The currently implemented correction scheme may result in errors (overcorrection) of up to 2-3% for the most eastward or westward ground pixels. The look-up table has been generated for a limited number of surface elevations (or surface pressures), covering the range 0-3 km in steps of 1 km. A simple next neighbor approach is currently implemented in order to select the reference spectra for a given ground pixel. This might result in retrieval errors which are 1% or larger, depending on spectral interval, ground pixel average surface elevation, etc. There are many other potential sources of retrieval errors which are not covered in this study (e.g., calibration errors). A potentially important error source which is difficult to quantify are the spectroscopic data (HITRAN[18] 2000 has been used for this study including all updates available until March 2003 and taking into account the pressure shift of line transitions not considered in earlier versions of the look-up table). Retrieval errors on the order of a few percent can be expected due to, e.g., line intensity uncertainties. In this context especially the low quality of the water lines for wavelength between 1700 and 2400 nm are noteworthy (as indicated by the quality flags given in HITRAN 2000), especially, because water absorption interferes with many CO_2, CH_4 and basically all CO lines in the spectral region observed by SCIAMACHY.

6. SPECTRAL FITS

Figures 5-8 show typical WFM-DOAS fit results corresponding to a scene over land (mid-west Africa, orbit 4700 from 23-Jan-2003, surface type vegetation/soil). The spectral absorption features of all major absorbers (CH_4, CO_2, O_2, and H_2O) are clearly visible. Each square symbol in Figs. 5-8 corresponds to one linear diode array detector pixel (gaps correspond to pixels which have not been used for retrieval (so called "dead" or "bad" pixels)). Note that so far CO_2 retrievals have been limited to the WIN_CH_6 fitting window. The retrieved columns including errors and root-mean-square (RMS) difference between measurement and model after the fit are listed in the figure captions. For low reflectivity scenes, e.g., over ocean outside sun-glint areas, the quality of the fit is typically worser (see bottom panels of Figs. 20-22). Ideally, the fit residuum should reflect the measurement noise. This limit, however, has not yet been reached. Currently, the fit residuals are on the order of the weak NIR absorbers CO and N_2O, which modulate the radiance by only approximately 1-3%. This is not due to measurement noise. The fit residuals are clearly dominated by systematic spectral features (as shown in Figure 9 for CO fits). Further investigation is needed to determine the reason for this (calibration, spectroscopy, etc.). Note that the residuals also depend (somewhat) on the spectrometer slit function assumed for the convolution of the reference spectra. In this study a Gaussian slit function has been used for channel 4 (Full Width at Half Maximum (FWHM): 0.415 nm) and channel 6 (1.4 nm) retrievals. For channel 8 a function of type $(a * (\lambda - \lambda_i)^b + 1)^{-1}$ has been used (with a equal to 0.24 and b equal to 2.7) resulting in slightly better fits than a Gaussian function (studies indicate that the channel 8 in-orbit line shape function deviates from the one determined on ground (Hans Schrijver (SRON), personal communication)). In one of the first WFM-DOAS studies[13] a "correction spectrum" has been determined and included in the fit to deal with systematic spectral artifacts. In comparison to that study the spectra used for this paper have an improved calibration with respect to dark signal correction and wavelength calibration (note that slight adjustments of the wavelength calibration are done as part of the WFM-DOAS retrieval using a spectral shift and squeeze algorithm).The SCIAMACHY nadir and solar spectra used in this study have been generated off-line by ESA to enable a better dark signal correction than possible with current operational processing. It is expected that SCIAMACHY spectra available in the near-future (after processor upgrade and reprocessing) will have a better quality as the spectra analyzed in this study. For this study no correction spectrum has been included in the fit. However, when investigating the retrieval results for this study, it was found that the columns of some gases are systematically under- or overestimated. This needs further investigation but uncertainties in the spectroscopic data might explain this at least partially. In order to make a preliminary first order correction for this, scaling factors have been applied to the retrieved columns reported in this study (as also done in similar studies[19,20]): all CO_2 columns have been multiplied by 1.05, all O_2 columns by 0.9, and all N_2O columns by 0.67. No scaling factors have been applied to CH_4, CO, and H_2O.

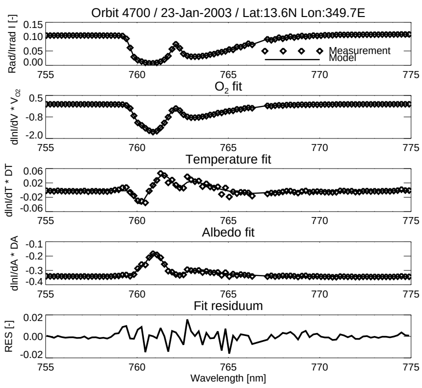

Fig. 5. Example for fit window WIN_CH_4. Retrieved O_2 column: $4.56 \cdot 10^{24}$ molecules/cm^2 ±0.5%. RMS fit residuum: 0.5%.

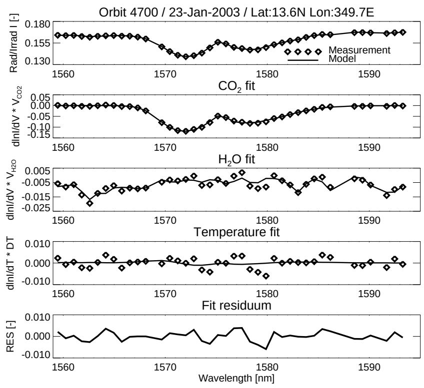

Fig. 6. Example for fit window WIN_CH_6. Retrieved CO_2 column: $7.82 \cdot 10^{21}$ molecules/cm^2 ±1.7%. RMS fit residuum: 0.2%.

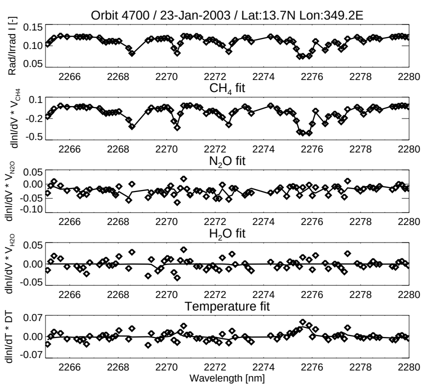

Fig. 7. Example for fit window WIN_CH_8a. CH_4 column: $3.83 \cdot 10^{19}$ molecules/cm^2 ±2.2%. N_2O: $6.3 \cdot 10^{18}$ molecules/cm^2 ±17%. RMS fit residuum: 1.2%.

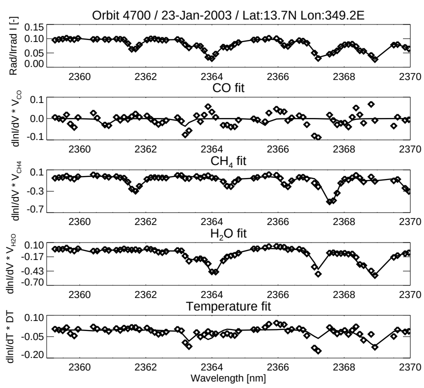

Fig. 8. Example for fit window WIN_CH_8b. CO column: $3.1 \cdot 10^{18}$ molecules/cm^2 ±43%. CH_4 column: $3.3 \cdot 10^{19}$ molecules/cm^2 ±4%. RMS fit residuum: 2.8%.

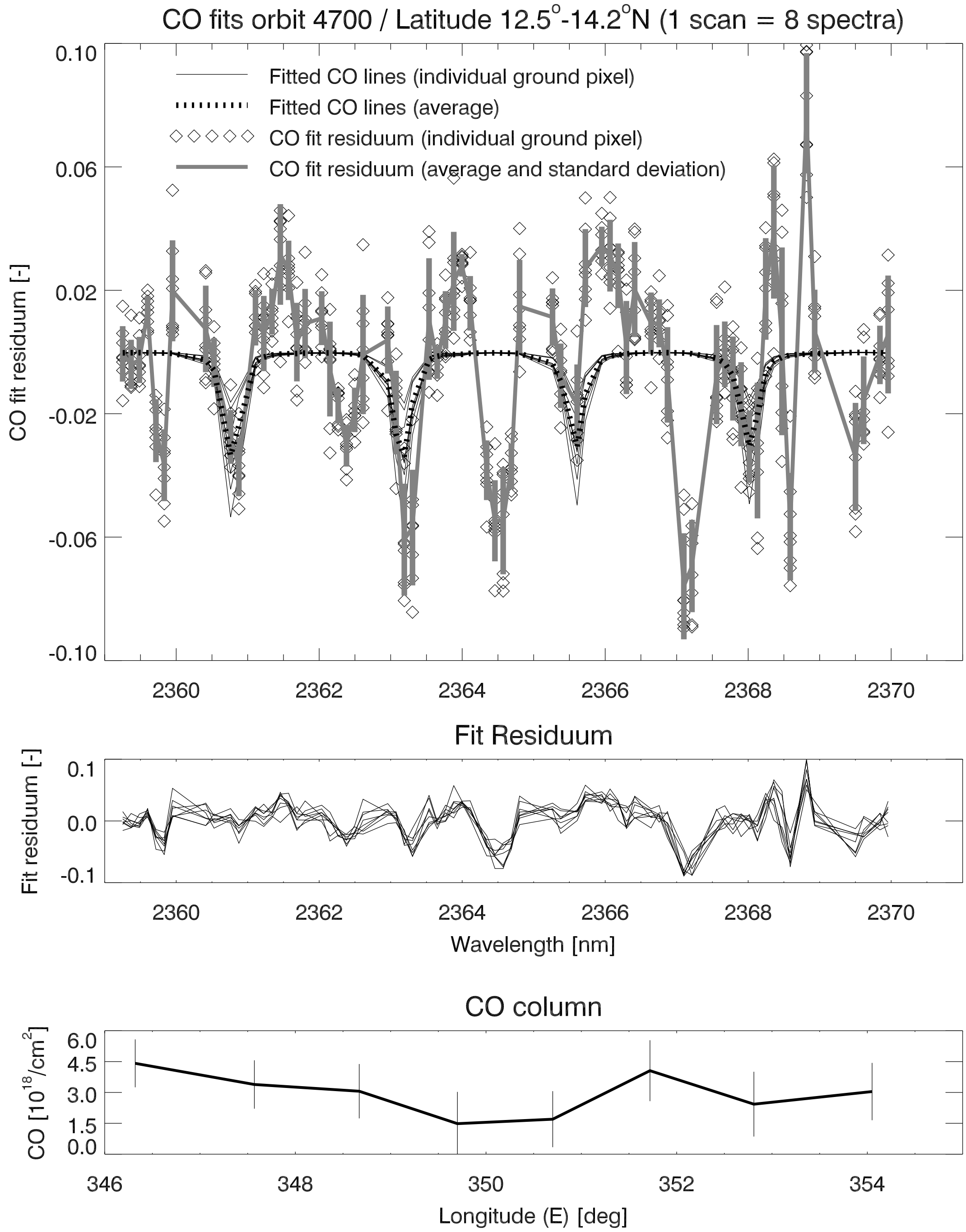

Fig. 9. CO spectral fit results from eight consecutive ground pixels corresponding to one east to west scan over mid-west Africa. Top: The thick grey line is the average "CO fit residuum" obtained from the eight individual CO fit residuals (symbols). The CO fit residuum is the sum of the fit residuum (model - measurement after fit, see also middle panel) plus fitted CO absorption (thin black lines (individual fits) and average of fitted CO lines shown as dotted thick line). The grey vertical lines denote one standard deviation of the CO fit residuals indicating approximately the measurement noise (1-2%). Bottom: Retrieved CO columns including fit error. The fit residuum (RMS approximately 3%) is dominated by still to be explained systematic spectral features on the order of the weak CO absorption lines.

7. WFM-DOAS PROCESSING OF ENTIRE ORBITS

In this section results from two orbits are presented and discussed (orbits 4700 and 4701 from 23-Jan-2003), starting with cloud issues. If clouds are inside the field-of-view of SCIAMACHY they might shield a significant amount of the total column. SCIAMACHY offers various means for cloud detection.[2] For this study a simple single threshold algorithm has been used to generate a cloud mask from SCIAMACHY's PMD (Polarization Measurement Device) measurements in the ultra-violet (PMD1). PMD1 detects a linear polarized component of the nadir radiance at low spectral (∼320-380 nm) but relatively high (in comparison to the main channels) spatial resolution of 7×30 km^2. PMD1 signals (after division by the cosine of the SZA) for orbits 4700 and 4701 are shown in Fig. 10. Well known cloud structures (corresponding to high PMD1 signals) are clearly visible. For the interpretation of the retrieval results the following information is of interest: For a surface pressure of 1013 hPa the columns (in molecules/cm^2) of the well-mixed gases CH_4, CO_2, and O_2 are approximately $3.8\cdot10^{19}$, $8.0\cdot10^{21}$, and $4.5\cdot10^{24}$, respectively. The variability of the CO_2 column is on the order of 3%.[15] In the following a CH_4 column variability of 5% is assumed, which also corresponds to the average inter-hemispheric difference. Figures 11-13 show O_2, CH_4, and CO_2 columns as retrieved from orbits 4700 (right) and 4701 (left). No cloud mask or cloud correction has been applied. As one would expect, low columns are clearly correlated with the cloud structures visible in Fig. 10. Because of the low variability of the gases discussed here it is interesting to note that a significant variability of the retrieved columns of all three gases in combination with a clear correlation is present also for apparently cloud free ground pixels (see also Figures 16 and 17). This is probably mainly due to two effects: (i) changes in surface pressure (or surface elevation) and (ii) albedo effects. The first effect corresponds to real column changes, the second might result from an algorithm limitation, namely the use of a single surface albedo (0.1) for the construction of the look-up table. Concerning (i): The correlation with surface elevation is most pronounced for the nadir measurements at 10-14°N latitude of orbit 4700 (the nadir "state" (i.e., rectangular block of nadir measurements) that covers parts of Senegal with apparently many cloud free pixels in combination with a significant variation of surface topography/elevation). Here, the average surface elevation of the ground pixels increases from nearly sea level (0 m) for west pixels to about 400 m for the direct nadir and east pixels. This should correspond to a column decrease from west to east of approximately 4% and this decrease is in fact visible in the retrieved columns (Fig. 18) demonstrating that SCIAMACHY is sensitive to even small CO_2 and CH_4 column changes on the order of one percent. Concerning (ii): Figures 11-13 show a relatively large variability of the retrieved columns for apparently cloud free measurements over the ocean, e.g., for the nadir state covering the 25-30°S latitude range of orbit 4700. Note that the very low columns (lower left corner of state colored in blue) are probably due to clouds (Fig. 10 shows some bright spots in this area). But even excluding these cloud contaminated pixels, the columns variability is still unrealistically high (up to 10-20%). This is probably related to changes in ocean reflectivity as a function of scan angle in combination with the albedo sensitivity of the presently implemented WFM-DOAS scheme. Note that for January the sun-glint condition (line of sight viewing direction close to direction of specular reflection of the direct sunlight) is fulfilled for the east pixels located between approximately 40°S latitude and the equator (each orbit). In this region higher (more realistic) columns are retrieved as compared to direct nadir pixels or west pixels. This dependency of the retrieved columns on the surface reflectivity (or albedo) is in accordance with the error analysis presented in section 5.3.

Figures 14 and 15 show CH_4 and CO_2 to O_2 column ratios (multiplied by 0.2095, the O_2 concentration of dry air) in the following also referred to as dry air column averaged mixing ratios XCH_4 and XCO_2, respectively. The XCO_2 errors have been calculated assuming uncorrelated fit errors of the corresponding CO_2 and O_2 columns, i.e., as root-sum-square of the CO_2 and O_2 errors (analog for XCH_4). Over Africa and over the ocean where the sun-glint condition is fulfilled, XCH_4 and XCO_2 are close to their expected values of 1780 ppbv and 370 ppmv, respectively, but outside these areas they show some (probably) unrealistic variability (see also Figs. 20 and 21). This can partly be explained by clouds not covered by the cloud mask (several bright spots in areas not covered by the cloud mask are visible when zooming into the PMD1 image). The low (O_2-normalized and not normalized) columns in mid and north Europe (Figures 11-15 and 20-21) might be related to relatively large solar zenith angles ($> 70°$) in January. Fig. 19 shows the temperature as retrieved from the CO_2 and O_2 fitting windows. Actually a temperature profile shift of the US Standard Atmosphere temperature profile has been retrieved. The temperatures shown in Fig. 19 are the temperature at the bottom of the US Standard Atmosphere plus the retrieved temperature shifts. Similar temperature shifts are retrieved from channel 8 retrievals but with significantly higher scattering. The latitude dependence of the temperature is roughly as one would expect for January (bell shaped curve centered around 20°S latitude with lower values towards higher latitudes). Fig. 19 shows the CO columns retrieved from orbit 4700 including the corresponding fit error, which is quite large reflecting the low quality of the spectral fit, especially over the ocean. The columns retrieved between 10°-35°N latitude are somewhat higher than the columns retrieved from MOPITT/EOS-Terra[21] (V3, L2V5.7.2.beta) on the same day, which are in the range 2-3·10^{18} molecules/cm^2 (see `http://www.eos.ucar.edu/mopitt/data/plots/mapsv3.html`).

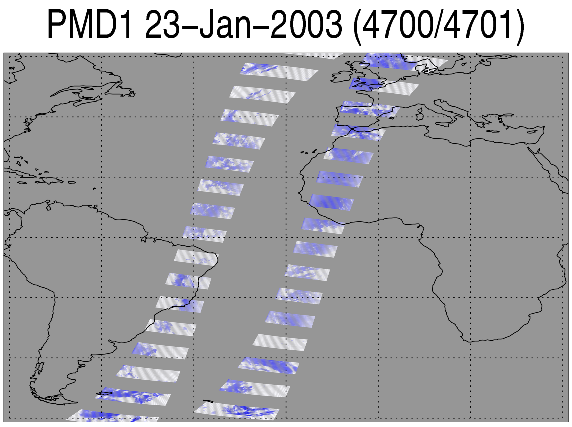

Fig. 10. SCIAMACHY PMD1 signal used for sub-pixel cloud identification (cloud mask see Figs. 14 and 15). Colors: low signal: dark blue, high signal: light blue/white (high probability for cloud in field of view).

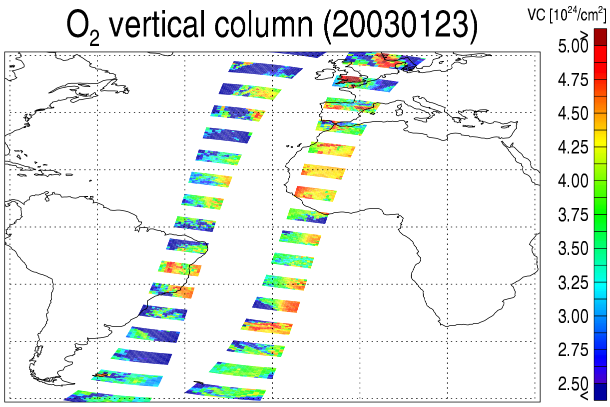

Fig. 11. O_2 vertical columns retrieved from orbit 4700 (right) and 4701 (left) from 23-Jan-2003 (fitting window WIN_CH_4). Each (colored) rectangular region corresponds to one nadir state (the gaps in between are due to the limb observations).

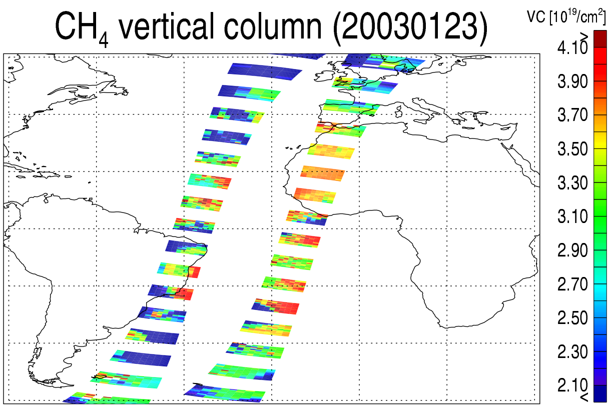

Fig. 12. As Fig. 11 but for CH_4 (window WIN_CH_8a).

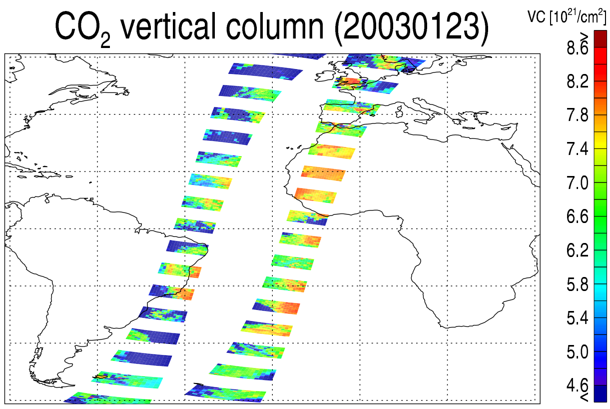

Fig. 13. As Fig. 11 but for CO_2 (window WIN_CH_6).

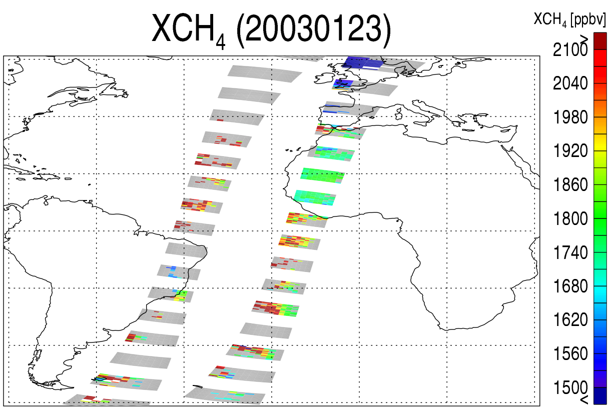

Fig. 14. XCH_4 derived from windows WIN_CH_8a (CH_4) and WIN_CH_4 (O_2). Here, the cloud mask has been applied (grey pixels).

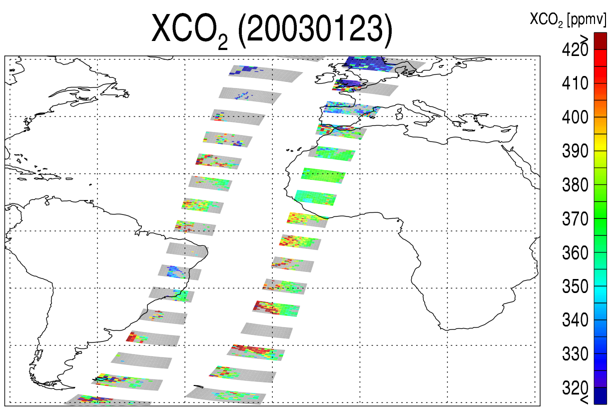

Fig. 15. XCO_2 derived from windows WIN_CH_6 (CO_2) and WIN_CH_4 (O_2). Here, the cloud mask has been applied (grey pixels).

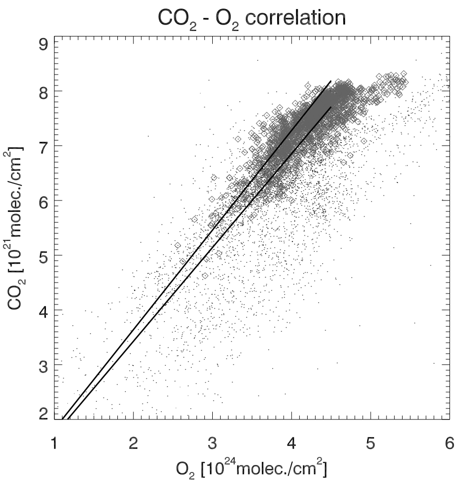

Fig. 16. CO_2 - O_2 column correlation. Tiny dots: all ground pixels from orbit 4700. Grey square symbols: subset of ground pixels (PMD1 < threshold (“cloud free”), XCO_2 error < 4%, SZA < 75°). The subset comprises 1759 out of 6927 pixels (25.4%). The two lines show the expected range of values assuming a ±3% variability of the CO_2 column assumed to be $7.95{\cdot}10^{21}$ molecules/cm^2 (370 ppmv) for an O_2 column of $4.5{\cdot}10^{24}$ molecules/cm^2.

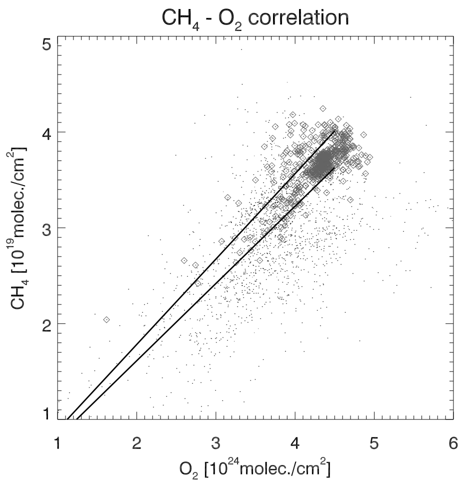

Fig. 17. CH_4 - O_2 column correlation. Tiny dots: all ground pixels from orbit 4700. Grey square symbols: subset of ground pixels (PMD1 < threshold (“cloud free”), XCH_4 error < 6%, SZA < 75°). The subset comprises 515 out of 2475 pixels (20.8%). The two lines show the expected range of values assuming a ±5% variability of the CH_4 column assumed to be $3.82{\cdot}10^{19}$ molecules/cm^2 (1780 ppbv) for an O_2 column of $4.5{\cdot}10^{24}$ molecules/cm^2.

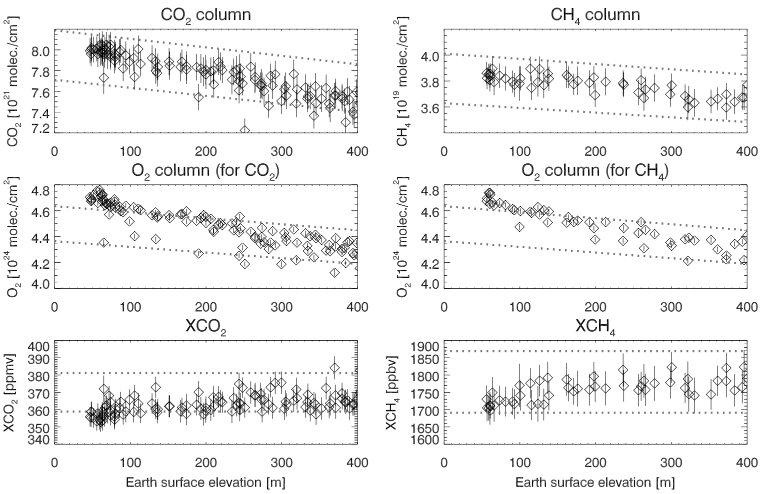

Fig. 18. CO_2, CH_4, and O_2 column correlation with ground pixel surface elevation. Only a subset of the ground pixels of orbit 4700 are shown here (located in latitude range 8°N-16°N / longitude range 340°-352°) corresponding to an apparently cloud free area with significant variation of the surface elevation. The dotted lines mark the assumed ±3% variability range for CO_2, O_2, and XCO_2 and ±5% for CH_4 and XCH_4 for the same mean columns (and mixing ratios) as listed in the captions of Figs. 16 and 17 (for sea level, i.e., 0 m). A linear decrease of the columns of 4% per 400 m altitude increase has been assumed (top and middle panels).

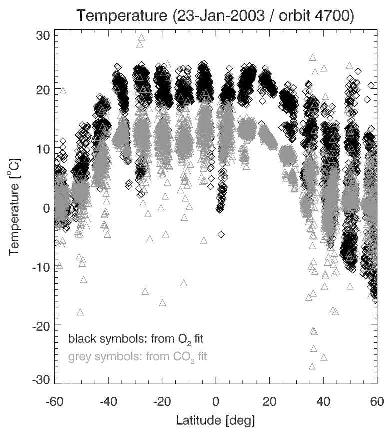

Fig. 19. Temperature as determined from fitting windows WIN_CH_4 (black symbols) and WIN_CH_6 (grey). They can be interpreted as temperatures at the bottom of the atmosphere (see main text for details). The results from all ground pixels are shown (e.g., including backscan pixel and without any cloud filtering).

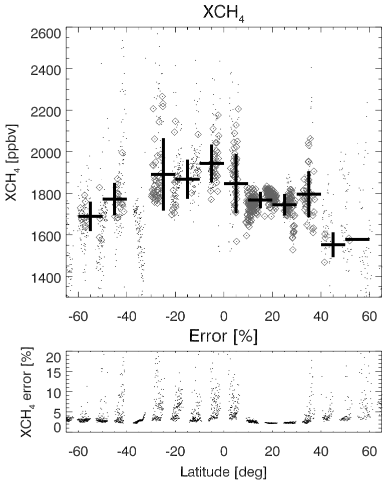

Fig. 20. XCH_4 (top) including 1-sigma error (bottom) for orbit 4700 (meaning of dots and square symbols: see Figs. 16 and 17). The thick horizontal lines denote the average value of the (normalized) columns plotted as square symbols within 10° latitude bands. The vertical lines indicate their standard deviation.

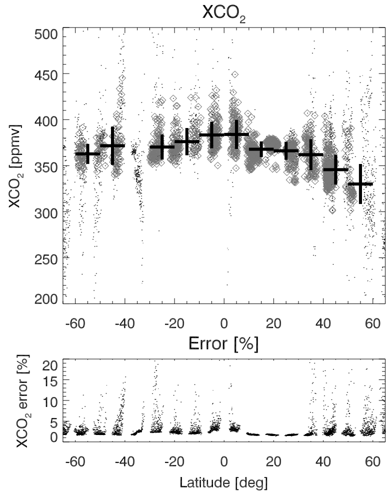

Fig. 21. As Figure 20 but for XCO_2. The solar zenith angle (SZA) at -60° latitude is ∼50° and at +60° latitude ∼80°. For the east pixels of each orbit located at -20° latitude the SZA has its minimum value of ∼25°.

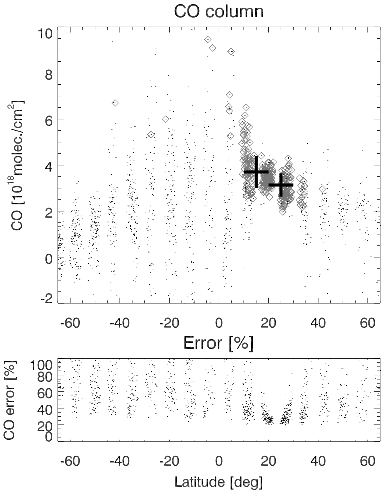

Fig. 22. As Figure 20 but for CO columns (here the error criterion for the subset is: CO fit error $<$ 50%). The average columns and standard deviations are only shown for latitude bands containing more than 15 data points (i.e., more than 15 square symbols).

CONCLUSIONS

A first version of the WFM-DOAS retrieval algorithm has been implemented based on a fast look-up table approach chosen to avoid time consuming on-line radiative transfer simulations. The algorithm and the look-up table has been described along with an initial error analysis based on simulated measurements. This analysis focuses on errors introduced by vertical profiles of trace gases and temperature which differ from the look-up table assumptions, aerosols, subvisual cirrus clouds, and albedo. This analysis reveals that the error of the currently implemented WFM-DOAS algorithm with respect to CH_4, CO, and CO_2 column retrieval is on the order of a few percent. This is acceptable for CO but needs further improvement for CO_2 and CH_4 to reach their significantly more challenging accuracy requirements. Weighting functions and averaging kernels show that the SCIAMACHY nadir measurements are highly sensitive to CH_4, CO, and CO_2 concentration changes even in the lowest kilometer of the atmosphere. First results have been presented obtained by applying this method to small spectral fitting windows focusing on CH_4, CO_2, CO, and O_2 column retrieval and CH_4 and CO_2 to O_2 column ratios. The retrieved columns have the right order of magnitude and show the expected correlation of the well mixed gases CO_2 and CH_4 with O_2 and surface topography. The standard deviation of the retrieved O_2 normalized CO_2 (CH_4) columns within 10° latitude bands is $\pm$10 ppmv ($\pm$50 ppbv) for measurements over land (over ocean the scatter is a factor of 2-4 larger). Especially the CO retrieval needs further study and improvement. The CO fit errors are 20-40% over land but typically significantly larger over the ocean. The CO fit residuals are dominated by relatively stable systematic artifacts (also present in the CO_2 and CH_4 spectral fitting windows) on the order of the weak CO absorption lines.

ACKNOWLEDGMENTS

This work has been funded by the BMBF via DLR-Bonn (Grants 50EE0027 and 50EE9901) and GSF/PT-UKF (Grant 07UFE12/8), the European Commission (Fifth Framework Programme on Energy, Environment and Sustainable Development, Contract no. EVG1-CT-2002-00079, project EVERGREEN), and by the University and the State of Bremen. We thank Johannes Frerick, ESTEC/ESA, for providing the SCIAMACHY spectra analyzed in this study. We also would like to thank our colleagues Stefan Noël and Klaus Bramstedt for providing us with the tools for reading the (binary) ENVISAT orbit files and our formerly colleague Michael Eisinger (now ESTEC/ESA) for the source code of the DOAS fitting software *kvant* which has been modified and used for this study.

REFERENCES

1. M. Buchwitz, V. V. Rozanov, and J. P. Burrows, “A near infrared optimized DOAS method for the fast global retrieval of atmospheric CH_4, CO, CO_2, H_2O, and N_2O total column amounts from SCIAMACHY / ENVISAT-1 nadir radiances,” *J. Geophys. Res.* **105**, pp. 15231–15246, 2000.
2. H. Bovensmann, J. P. Burrows, M. Buchwitz, J. Frerick, S. Noël, V. V. Rozanov, K. V. Chance, and A. Goede, “SCIAMACHY - mission objectives and measurement modes,” *J. Atmos. Sci.* **56**, pp. 127–150, 1999.
3. J. P. Burrows, M. Weber, M. Buchwitz, V. V. Rozanov, A. Ladstätter-Weißenmayer, A. Richter, R. de Beek, R. Hoogen, K. Bramstedt, K.-U. Eichmann, and M. Eisinger, “The Global Ozone Monitoring Experiment (GOME): Mission concept and first scientific results,” *J. Atmos. Sci.* **56**, pp. 151–175, 1999.
4. A. G. Straume et al., “Verification of CO, CH_4, and CO_2 total columns from the SCIAMACHY near-infrared channels,” in *Proceedings of the ENVISAT Validation Workshop*, **SP-531**, 2002.
5. C. Frankenberg et al., “SCIAMACHY NIR-channels: Retrieval and preliminary results.” EGS-AGU-EUG Joint Assembly, Nice, France, 6-11 April (poster presentation), 2003.
6. A. Stepnik et al., “Extracting column densities of CO_2 from ENVISAT/SCIAMACHY.” EGS-AGU-EUG Joint Assembly, Nice, France, 6-11 April (poster presentation), 2003.
7. H. Schrijver, A. P. H. Goede, M. R. Dobber, and M. Buchwitz, “Retrieval of carbon monoxide, methane and nitrous oxide from SCIAMACHY measurements,” in *Optical Remote Sensing of the Atmosphere and Clouds*, J. Wang, B. Wu, T. Ogawa, and Z. Guan, eds., *Proc. SPIE* **3501**, pp. 215–224, 1998. Beijing, China, 14-17 Sept. 1998.
8. S. Houweling, T. Kaminski, F. Dentener, J. Lelieveld, and M. Heimann, “Inverse modeling of methane sources and sinks using the adjoint of a global transport model,” *J. Geophys. Res.* **104**, pp. 26137–26160, 1999.
9. D. M. O’Brian and P. J. Rayner, “The utility of remotely sensed CO_2 concentration data in surface source inversions,” *Geophys. Res. Let.* **28**, pp. 175–178, 2001.
10. Z. Kuang, J. S. Margolis, G. C. Toon, D. Crisp, and Y. Yung, “Spaceborn measurements of atmospheric CO_2 by high-resolution NIR spectrometry of reflected sunlight: An introductory study,” *Geophys. Res. Let.* **29**(10.1029/2001GL014298), 2002.
11. M. Buchwitz, V. V. Rozanov, and J. P. Burrows, “A correlated-k distribution scheme for overlapping gases suitable for retrieval of atmospheric constituents from moderate resolution radiance measurements in the visible/near-infrared spectral region,” *J. Geophys. Res.* **105**, pp. 15247–15262, 2000.
12. W. Press, S. Teukolsky, W. Vetterling, and B. Flannery, *Numerical Recipes in Fortran*, Cambridge University Press, London, 1992.
13. M. Buchwitz, V. V. Rozanov, and J. P. Burrows, “Retrieval of trace gas vertical columns from SCIAMACHY/ENVISAT near-infrared nadir spectra: First preliminary results,” *Adv. Space Res. (in press)* , 2003.
14. R. M. Goody and Y. L. Yung, *Atmospheric Radiation*, Oxford University Press, New York, 1989.
15. E. Dufour and F.-M. Bréon, “Spaceborn estimate of atmospheric CO_2 column by use of the differential absorption method: error analysis,” *Applied Optics* **42**, pp. 3595–3609, 2003.
16. E. P. Shettle and R. W. Fenn, “Models of the aerosols of the lower atmosphere and the effects of humidity variations on their optical properties,” tech. rep., Air Force Geophys. Lab. AFGL, 1979.
17. M. Hess, P. Koepke, and I. Schult, “Optical properties of aerosols and clouds: The software package OPAC,” *Bulletin of the American Meteorological Society* **75**, pp. 831–844, 1998.
18. L. S. Rothman, C. P. Rinsland, A. Goldman, S. T. Massie, D. P. Edwards, J.-M. Flaud, A. Perrin, C. Camy-Peyret, V. Dana, J.-Y. Mandin, J. Schroeder, A. McCann, R. R. Gamache, R. B. Wattson, K. Yoshino, K. V. Chance, K. W. Jucks, L. R. Brown, V. Nemtchinov, and P. Varanasi, “The HITRAN molecular spectroscopic database and HAWKS (HITRAN atmospheric workstation): 1996 edition,” *J. Quant. Spectrosc. Radiat. Transfer* **60 (5)**, pp. 665–710, 1998.
19. Z. H. Yang, G. C. Toon, J. S. Margolis, and P. O. Wennberg, “Atmospheric CO_2 retrieved from ground-based near IR solar spectra,” *Geophys. Res. Let.* **29**(10.1029/2001GL014537), 2002.
20. E. Dufour and F.-M. Bréon, “Ground based inversion of CO_2 column densities from solar spectra,” *J. Geophys. Res. (submitted)* , 2003.
21. M. N. Deeter, L. K. Emmons, G. L. Francis, D. P. Edwards, J. C. Gille, J. X. Warner, B. Khattatov, D. Ziskin, J.-F. Lamarque, S.-P. Ho, V. Yuding, J.-L. Attie, D. Packman, J. Chen, D. Mao, and J. R. Drummond, “Operational carbon monoxide retrieval algorithm and selected results for the MOPITT instrument,” *J. Geophys. Res. (in press)* , 2003.